

# Theory of the undulating magnetic ground state of cylindrical cobalt nanowires

R. P. Erickson\*

*National Institute of Standards and Technology, Boulder, Colorado 80305, USA*

D. L. Mills

*Department of Physics and Astronomy, University of California, Irvine, California 92697, USA*

(Received 18 September 2009; published 11 December 2009)

In cylindrical Co nanowires it is possible for the easy axis to lie in the plane perpendicular to their symmetry axis. The ground state realized is then the result of the competition between shape anisotropy, which favors ferromagnetism with moment parallel to the symmetry axis and anisotropy along the easy axis. Recent experiments show an undulating state of magnetization can then result. We discuss the magnetic phase diagram of such nanowires, and we present a theory of the undulating state, which we refer to as the snake state.

DOI: [10.1103/PhysRevB.80.214410](https://doi.org/10.1103/PhysRevB.80.214410)

PACS number(s): 75.25.+z, 75.30.Gw

## I. INTRODUCTION

The study of magnetic nanostructures has been a very active topic of research for many years now. In such structures, one encounters new physics not present in bulk materials,<sup>1</sup> and at the same time magnetic nanostructures are utilized in devices. The development of giant magnetoresistance read heads<sup>2</sup> have revolutionized magnetic data storage technology, for example.

The nature of the ground state realized in ferromagnetic nanostructures can be varied or controlled by means not realized in bulk magnetic materials. For instance, consider ultrathin ferromagnet films. In such films of Ni grown on Cu(100), whether the magnetization lies in plane or perpendicular to the film surfaces can be controlled by the film thickness.<sup>3</sup> Also, by tuning the temperature in ultrathin films for a given film/substrate combination one may also realize either perpendicular or parallel orientation of the film magnetization.<sup>4</sup> In ultrathin films, surface and interface anisotropy can be so strong that it overwhelms the shape anisotropy, with origin in the dipolar interactions. The latter favors the in-plane state. Through variation in the substrate on which the film is grown, or the growth conditions, one may realize either perpendicular or parallel orientation of the magnetization in a film formed from a particular material. The frequencies of the dynamic response of the spins in such materials can be varied over a considerable range as well since these are influenced strongly by material properties such as surface and shape anisotropy in addition to the nature of the ground state itself. Thus, in ultrathin films one can design magnetic materials with a wide range of desirable properties.

Ferromagnetic nanowires have been explored extensively as well. High-quality nanowires of cylindrical cross section can be fabricated by growing them in materials that contain cylindrical channels.<sup>5</sup> Shape anisotropy aligns the magnetization parallel to the symmetry axis of the nanowire in such samples, though application of an external magnetic field can cant the magnetization with respect to the symmetry axis. In fact one can orient the magnetization perpendicular to the symmetry axis by such an external field.<sup>5</sup>

A number of groups have recently grown and characterized long Co nanowires of cylindrical cross section,<sup>6–12</sup>

through electrodeposition into pores in membranes.<sup>13</sup> These wires have fascinating properties. If their radius is sufficiently small, below approximately 20 nm, atomic force microscopy studies show the ground state consists of a single domain, with moment aligned parallel to the symmetry axis of the wire.<sup>10</sup> In the thicker wires, the hcp crystal structure is found with  $c$  axis in the plane perpendicular to the symmetry axis. This suggests the easy axis associated with magnetocrystalline anisotropy lies in this plane, parallel to the  $c$  axis.<sup>9</sup> In a number of studies in such wires, AFM images reveal domain patterns.

In a recent experimental study of a Co nanowire with a radius of 45 nm, AFM images<sup>12</sup> show the ground state to be a periodic, modulated structure with the rather long period of 700 nm. Bergmann and collaborators<sup>14</sup> suggested that an undulating state is the ground state, and by means of a variational calculation they demonstrated that such a state has lower energy than a simple ferromagnetic state. Suppose the  $z$  axis is the symmetry axis of the wire, and the easy axis lies perpendicular to this, in the  $x$  direction. These authors proposed that in the ground state, the magnetization has the form  $M_z = M_S \cos[\theta_0 \sin(kz)]$ ,  $M_x = M_S \sin[\theta_0 \sin(kz)]$ , and  $M_y = 0$ . Their variational procedure demonstrated there is an energy minimum for appropriate values of  $\theta_0$  and  $k$ . The period that emerges from their analysis is roughly three times the wire radius, for parameters characteristic of bulk ferromagnetic Co. This is much smaller than the experimental value of the ground-state period, which is 15.5 wire radii, it might be noted. In what follows, we shall refer to such a ground state as a “snake state” since the ground-state magnetization undulates in a snakelike manner as one proceeds down the symmetry axis of the wire.

The ground state suggested by the authors of Ref. 14 is intriguing. For example, if this is indeed the state realized in Co nanowires with radii in excess of 20 nm or so, then it should be possible to tune or alter the period or character of the state by application of a modest magnetic field. Spin-wave propagation in such a periodic structure should be of great interest since its periodic character will introduce gaps in the spin-wave dispersion relation; it is quite possible that the dispersion relation and nature of the gaps could be tuned through application of an external magnetic field. Such a

possibility should be of great interest from the point of view of device applications.

The purpose of this paper is to present an exact description of the snake state, within the framework of the assumption that the magnetization per unit volume depends only on the coordinate  $z$  introduced above. We derive a rather simple form for the energy functional that describes the state in which the magnetization is defined by  $M_z = M_S \cos[\theta(z)]$ ,  $M_x = M_S \sin[\theta(z)]$ , and  $M_y = 0$ , where  $\theta(z)$  is periodic with period  $L$ . A variational procedure leads us to an integrodifferential equation (an Euler Lagrange equation) satisfied by those forms  $\theta(z)$  that produce an extremum in the energy functional. We can prove that the Ansatz for  $\theta(z)$  proposed in Ref. 14 emerges from our analysis in the near-threshold regime. A linearization procedure leads us to a criterion from which one can obtain the critical value of the anisotropy required to render the simple ferromagnetic state unstable with respect to the snake state, along with its period at the onset of the instability. We then proceed to describe the snake state well beyond threshold, through numerical solutions of the integrodifferential equation. We find that the Ansatz employed in Ref. 14 applies only very near threshold; beyond this our picture is very different. One realizes domains inside of which the magnetization is canted with respect to the symmetry axis, separated by domains whose character is outlined below. Physically reasonable values of the anisotropy can produce periodic ground states whose period is as long as found experimentally in Ref. 12.

This paper is organized as follows. In Sec. II, we derive the basic Euler Lagrange equation which forms the core of our analysis, discuss the information we can extract from it near the instability threshold, and also comment on the numerical methods we have used to solve it. In Sec. III we discuss the results of our numerical studies and Sec. IV is devoted to concluding remarks.

## II. THEORY

We shall consider an infinitely long ferromagnetic nanowire of cylindrical cross section, with radius  $R$ . The  $z$  axis coincides with the symmetry axis of the wire. We assume that the wire is sufficiently thin that, to good approximation, the magnetization per unit volume  $\vec{M}(\vec{r})$  in the ground state can be supposed to depend only on the coordinate  $z$ . The  $x$  axis, perpendicular to the symmetry axis of the wire, will be assumed to be the easy axis, from the point of view of the magnetocrystalline anisotropy. We follow the authors of Ref. 14 by assuming that in the ground state, the magnetization lies in the  $xz$  plane. Thus, we write the ground-state magnetization in the form

$$\vec{M}(\vec{r}) = M_S [\hat{x} \sin \theta(z) + \hat{z} \cos \theta(z)]. \quad (1)$$

Our task will be to find the form of  $\theta(z)$  which minimizes the ground-state energy. For the moment, we let  $\theta(z)$  be general, though later on we will assume it is periodic with a period  $L$ , also to be determined by requiring the energy to be a minimum. When  $\theta(z)$  is periodic, the magnetization undulates in a snakelike manner as one moves down the wire. For this

reason we refer to this state as a snake state, as mentioned in Sec. I.

The ground-state energy functional of the nanowire will be written in the form

$$E(\{\vec{M}(\vec{r})\}) = \int_V d^3r \left\{ \frac{A}{M_S^2} \sum_{\alpha=x,y,z} |\vec{\nabla} M_\alpha(\vec{r})|^2 - \frac{K_1}{M_S^2} M_x(\vec{r})^2 - \frac{K_2}{M_S^4} M_x(\vec{r})^4 - \frac{1}{2} \vec{H}_{dip}(\vec{r}) \cdot \vec{M}(\vec{r}) - \vec{H}_0 \cdot \vec{M}(\vec{r}) \right\}. \quad (2)$$

The first term is the exchange energy, the second and third terms are the magnetocrystalline anisotropy, the fourth term is the dipolar energy, and the last term is the interaction of the magnetization with an externally applied Zeeman field. We shall assume that  $\vec{H}_0 = H_0 \{\hat{x} \sin \theta_H + \hat{z} \cos \theta_H\}$ . We also suppose that  $K_1 > 0$  and  $K_1 > |K_2|$  so the  $x$  axis is an easy axis. The reader should note that the convention we use here to describe the magnetocrystalline anisotropy differs from that employed in Ref. 14. These authors write the crystalline anisotropy in the form  $(k_1/M_S^2)M_z(\vec{r})^2 + (k_2/M_S^4)M_z(\vec{r})^4$ . It is easy to see that one has the correspondence  $K_1 \leftrightarrow k_1 + 2k_2$  and  $K_2 \leftrightarrow -k_2$ .

Our attention will be directed toward the dipolar field. There are two contributions to  $\vec{H}_{dip}(\vec{r})$ , one from surface magnetic charges and one from volume charges. We refer to these as  $\vec{H}_{dip}^{(S)}(\vec{r})$  and  $\vec{H}_{dip}^{(V)}(\vec{r})$ , respectively. One has, in notation appropriate to a cylindrical coordinate system,

$$\begin{aligned} \vec{H}_{dip}^{(S)}(\vec{r}) &= -\vec{\nabla} \int_S dS' \frac{\hat{\rho}' \cdot \vec{M}(\vec{r}')}{|\vec{r} - \vec{r}'|} \\ &= -RM_S \vec{\nabla} \int_{-\infty}^{+\infty} dz' \int_0^{2\pi} d\phi' \frac{\sin \theta(z') \cos \phi'}{\sqrt{|\vec{\rho} - R\hat{\rho}'|^2 + (z - z')^2}} \end{aligned} \quad (3a)$$

and

$$\begin{aligned} \vec{H}_{dip}^{(V)} &= \vec{\nabla} \int_V d^3r' \frac{\nabla' \cdot \vec{M}(\vec{r}')}{|\vec{r} - \vec{r}'|} \\ &= -M_S \vec{\nabla} \int_{-\infty}^{+\infty} dz' \int_0^R d\rho' \rho' \int_0^{2\pi} d\phi' \\ &\quad \times \frac{\dot{\theta}(z') \sin \theta(z')}{\sqrt{|\vec{\rho} - \vec{\rho}'|^2 + (z - z')^2}}, \end{aligned} \quad (3b)$$

where  $\dot{\theta}(z) = d\theta(z)/dz$ . We shall use the identity

$$\begin{aligned} \frac{1}{\sqrt{|\vec{\rho} - \vec{\rho}'|^2 + (z - z')^2}} &= \frac{1}{2\pi} \int d^2k_{\parallel} \exp[i\vec{k}_{\parallel} \cdot (\vec{\rho} - \vec{\rho}')] \\ &\quad - k_{\parallel} |z - z'|. \end{aligned} \quad (4)$$

After some algebra, this identity allows us to write the dipolar fields in the form

$$\vec{H}_{dip}^{(S)}(\vec{r}) = -2\pi M_S R \vec{\nabla} \left\{ \cos \phi \int_0^\infty dk_\parallel J_1(k_\parallel R) J_1(k_\parallel \rho) \right. \\ \left. \times \int_{-\infty}^{+\infty} dz' \sin \theta(z') \exp[-k_\parallel |z - z'|] \right\} \quad (5a)$$

and

$$\vec{H}_{dip}^{(V)}(\vec{r}) = -2\pi M_S R \vec{\nabla} \left\{ \int_0^\infty \frac{dk_\parallel}{k_\parallel} J_1(k_\parallel R) J_0(k_\parallel \rho) \right. \\ \left. \times \int_{-\infty}^{+\infty} dz' \dot{\theta}(z') \sin \theta(z') \exp[-k_\parallel |z - z'|] \right\}. \quad (5b)$$

An integration by parts in Eq. (5b) leads to

$$\vec{H}_{dip}^{(V)} = -2\pi M_S R \vec{\nabla} \left\{ \int_0^\infty dk_\parallel J_1(k_\parallel R) J_0(k_\parallel \rho) \right. \\ \left. \times \int_{-\infty}^{+\infty} dz' \cos \theta(z') \operatorname{sgn}(z - z') \exp[-k_\parallel |z - z'|] \right\}. \quad (5c)$$

When these forms are inserted into the dipolar contribution to the energy functional in Eq. (2), we find, changing notation a bit,

$$E[\theta(z)] = \pi R^2 \int_{-\infty}^{+\infty} dz \{ A \dot{\theta}(z)^2 - K_1 \sin^2 \theta(z) - K_2 \sin^4 \theta(z) \\ - M_S H_0 \cos[\theta(z) - \theta_H] \} + E_{Dip}[\theta(z)], \quad (6a)$$

where the dipolar contribution to the energy functional can be written as

$$E_{Dip}[\theta(z)] = \pi^2 R^2 M_S^2 \int_{-\infty}^{+\infty} dz \left\{ 2 \cos^2 \theta(z) \right. \\ \left. - \int_{-\infty}^{+\infty} dz' D(z - z'; R) [2 \cos \theta(z) \cos \theta(z') \right. \\ \left. - \sin \theta(z) \sin \theta(z')] \right\} \quad (6b)$$

with

$$D(x; R) = \int_0^\infty dk J_1(kR)^2 e^{-k|x|}. \quad (6c)$$

Our task is to seek functions  $\theta(z)$  that minimize the energy functional in Eq. (6). We shall proceed by generating an Euler Lagrange equation obtained by setting the functional derivative  $\delta E[\theta(z)]/\delta \theta(z')$  to zero. This is a straightforward exercise. However, if we proceed with Eq. (6) as it stands, the task of solving the Euler Lagrange equation numerically is challenging. It has the form of an integrodifferential equation with a nonlocal term that contains the kernel  $D(z - z'; R)$ . This has a logarithmic singularity as  $z'$  approaches  $z$ . We can remove this difficulty as follows. We introduce a new function  $\Gamma(z - z'; R)$  defined by the statement

$$\Gamma(z - z'; R) = \int_{-\infty}^{z-z'} dz'' D(z'', R), \quad (7)$$

which means that we may also write  $\partial \Gamma(z - z'; R)/\partial z' = -D(z - z'; R)$ . One finds

$$\Gamma(z - z'; R) = \Theta(z - z') - g(z - z'; R),$$

where  $\Theta(x)$  is the Heaviside step function and

$$g(z - z'; R) = \operatorname{sgn}(z - z') \int_0^\infty \frac{du}{u} J_1(u)^2 \exp[-u|z - z'|/R]. \quad (8)$$

Note that the integral in  $g(z - z'; R)$  is finite as  $z' \rightarrow z$ . An exercise in partial integration yields the identity

$$\int_{-\infty}^{+\infty} D(z - z'; R) f[\theta(z), \theta(z')] dz' \\ = f[\theta(z), \theta(z)] - \int_{-\infty}^{+\infty} g(z - z'; R) \frac{\partial f[\theta(z), \theta(z')]}{\partial \theta(z')} \dot{\theta}(z') dz', \quad (9)$$

where again  $\dot{\theta}(z') = d\theta(z')/dz'$ . The dipolar contribution to the energy functional now has the form

$$E_{Dip}[\theta(z)] = \pi^2 R^2 M_S^2 \int_{-\infty}^{+\infty} dz \left\{ \sin^2 \theta(z) - \int_{-\infty}^{+\infty} dz' g(z - z'; R) \right. \\ \left. \times [2 \sin \theta(z') \cos \theta(z) \right. \\ \left. + \cos \theta(z') \sin \theta(z)] \dot{\theta}(z') \right\}. \quad (10)$$

The Euler Lagrange equation associated with the energy functional derived above can be written as

$$A \ddot{\theta}(z) + \frac{1}{2} (K_1 - \pi M_S^2) \sin 2\theta(z) + K_2 \sin^2 \theta(z) \sin 2\theta(z) \\ - \frac{1}{2} M_S H_0 \sin[\theta(z) - \theta_H] + \pi M_S^2 \int_{-\infty}^{+\infty} dz' g(z - z'; R) \\ \times [2 \sin \theta(z') \sin \theta(z) + \cos \theta(z') \cos \theta(z)] \dot{\theta}(z') = 0. \quad (11)$$

Our interest will be centered on the case where  $\theta(z)$  is periodic with period  $L$ ; in our numerical studies the period will be determined by minimizing the energy per unit length of the system. We conclude by quoting the form of the energy functional and the Euler Lagrange equation for this case. We center a unit cell around  $z=0$  so it extends from  $z=-L/2$  to  $z=+L/2$ . We measure length in units of  $x=2z/L$ . We also suppose the nanowire consists of a very large number of unit cells whose number is  $N+1$ . It is then possible to reduce all integrals in Eqs. (10) and (11) to integrals over just the unit cell that surrounds the origin of the coordinate system. Of interest will be the energy per unit length per unit area of the system. We introduce the dimensionless energy density

$e[\theta(x)] = E[\theta(z)]/2\pi M_S^2 R^2 L(N+1)$ , which may be cast into the form

$$e[\theta(x)] = \int_{-1}^{+1} dx \left\{ \frac{h_A}{2l^2} \dot{\theta}(x)^2 - \frac{h_K}{2} [1 + \kappa \sin^2 \theta(x)] \sin^2 \theta(x) + \frac{1}{4} \sin^2 \theta(x) - h_0 \cos[\theta(x) - \theta_H] \right\} + e_{nl}[\theta(x)], \quad (12a)$$

where the nonlocal term is

$$e_{nl}[\theta(x)] = \frac{1}{4} \int_{-1}^{+1} dx \int_{-1}^{+1} dx' \tilde{g}(x-x'; l) [2 \sin \theta(x') \cos \theta(x) + \sin \theta(x) \cos \theta(x')] \dot{\theta}(x'). \quad (12b)$$

All quantities in Eq. (12) are dimensionless. We have  $h_A = 2A/\pi R^2 M_S^2$  as a measure of the strength of the exchange,  $l = L/R$ ,  $h_K = K_1/2\pi M_S^2$  as a measure of the first-order anisotropy,  $\kappa = K_2/K_1$  and  $h_0 = H_0/4\pi M_S$ . Recall that the dimensionless measure of length is  $x = 2z/L$ . Finally the nonlocal kernel, once this term is reduced to an integral only over the unit cell surrounding the origin, is

$$\tilde{g}(x) = \text{sgn}(x) \int_0^\infty \frac{du}{u} J_1(u)^2 \frac{\sinh\left[\frac{lu}{2}(|x|-1)\right]}{\sinh\left(\frac{lu}{2}\right)}. \quad (13)$$

The Euler Lagrange equation generated from the energy functional as written in Eq. (12) has the form

$$\frac{h_A}{l^2} \ddot{\theta}(x) + \frac{1}{2} \left\{ h_K [1 + 2\kappa \sin^2 \theta(x)] - \frac{1}{2} \right\} \sin 2\theta(x) - h_0 \sin[\theta(x) - \theta_H] + \frac{1}{2} \int_{-1}^{+1} dx' \tilde{g}(x-x'; l) \times [2 \sin \theta(x') \sin \theta(x) - \cos \theta(x') \cos \theta(x)] \dot{\theta}(x') = 0. \quad (14)$$

In Sec. III we turn to our numerical studies of the nature of the ground state generated from the formalism developed in this section.

### III. NUMERICAL STUDIES OF THE GROUND STATE

In this section, we describe our numerical studies of the nature of the ground state of the system, based on the use of Eq. (14) and also the energy functional stated in Eq. (12).

We begin our discussion with comments on the analysis presented earlier by Bergmann and his colleagues in Ref. 14. As discussed above, these authors carried out a variational analysis of the nature of the ground state. This was done within a framework, in the present notation, that assumes  $\theta(z) = \theta_0 \sin(2\pi z/L)$ . Both  $\theta_0$  and  $L$  are treated as variational parameters, chosen to minimize the total energy. Their computation proceeds by a very different mathematical approach from ours, we should remark. It is our view that the energy

functional in Eq. (12) above is far more compact and easier to employ than that used in Ref. 14. Bergmann *et al.* chose two parameter sets for their analysis, based on the properties of bulk ferromagnetic Co metal. When we employ their Ansatz and carry out a variational analysis using the energy functional in Eq. (12), we reproduce the results quoted in their paper.

The next question is whether the Ansatz introduced in Ref. 14 is a reasonable description of the snake state. We can prove that their form for  $\theta(z)$  can be derived from our analysis in the limit that the angular deviation from the ferromagnetic state (with magnetization parallel to the symmetry axis) is small. To see that this is so, we employ the form of the Euler Lagrange equation displayed in Eq. (11). When this is linearized for small-angle deviations from the ferromagnetic state one finds

$$A \ddot{\theta}(z) + [K_1 - \pi M_S^2] \theta(z) + \pi M_S^2 \int_{-\infty}^{+\infty} dz' g(z-z'; R) \dot{\theta}(z') = 0. \quad (15)$$

It is easy to see that  $\theta(z) = \theta_0 \sin(2\pi z/L)$  is a solution of Eq. (15) provided that the period  $L$  is determined from the implicit relation

$$A \left( \frac{2\pi}{L} \right)^2 = K_1 - 2\pi M_S^2 \bar{K}_1 \left( \frac{2\pi R}{L} \right) \bar{I}_1 \left( \frac{2\pi R}{L} \right), \quad (16a)$$

where  $\bar{I}_1(x)$  and  $\bar{K}_1(x)$  are the modified Bessel functions of the first and second kind, respectively. We can write Eq. (16a) in terms of the dimensionless variables introduced in Sec. II, just above Eq. (13). One has

$$\frac{1}{l^2} = \frac{1}{\pi^2 h_A} \left[ h_K - \bar{K}_1 \left( \frac{2\pi}{l} \right) \bar{I}_1 \left( \frac{2\pi}{l} \right) \right]. \quad (16b)$$

Notice that the second-order anisotropy constant  $K_2$ , or equivalently  $\kappa$ , does not enter Eq. (16). The onset of the instability of the ferromagnetic state is controlled only by  $K_1$ , i.e.,  $h_K$ .

If we use the value of the experimental exchange stiffness for bulk Co quoted by the authors of Ref. 14, see below, then our parameter  $h_A = 0.0542$ . For this value of the exchange strength, a numerical solution of Eq. (16b) then shows that the uniform ferromagnetic state with moment parallel to the symmetry axis of the wire becomes unstable for  $h_K > 0.27$ . Right at the transition, one finds  $l = 2.57$ . At the transition, the period of the snake state is not so far from the value determined in Ref. 14.

We next turn to our numerical studies of the solutions of the full Euler Lagrange equation. Before we turn to the results, we discuss our choice of numerical parameters. We follow the authors of Ref. 14 for many of these. Little is known about the magnetic properties of the Co nanowires in which the easy axis is perpendicular to the symmetry axis of the nanowire so it is reasonable to use numbers appropriate to bulk Co. Thus, we choose  $4\pi M_S = 1.73$  T so that  $4\pi M_S^2 = 2.39 \times 10^6$  J/m<sup>3</sup>. For bulk Co, the experimental value of the exchange stiffness  $D = 6.96 \times 10^{-40}$  J m<sup>2</sup>, and we have  $D = 2g\mu_B A/M_S$  so that  $A = 2.59 \times 10^{-11}$  J/m. In all of our

calculations, again following Ref. 14, we take the radius of the wire to be  $R=40$  nm. Then our parameter  $h_A=0.0542$ , as mentioned in the previous paragraph. This value is used in all calculations reported below. As mentioned in Sec. I, our anisotropy constants  $K_1, K_2$  are related to those  $k_1, k_2$  used in Ref. 14 by  $K_1=k_1+2k_2$  and  $K_2=-k_2$ . For bulk Co,  $k_1=4.1 \times 10^5$  J/m<sup>3</sup>, and two values for  $k_2$  are quoted in Ref. 14,  $k_2=1.0 \times 10^5$  J/m<sup>3</sup> and  $k_2=1.5 \times 10^5$  J/m<sup>3</sup>. Thus for these two choices  $K_1=6.1 \times 10^5$  J/m<sup>3</sup> and  $K_1=7.1 \times 10^5$  J/m<sup>3</sup>. For these choices of  $K_1$ , our dimensionless parameter  $h_K$  assumes the values 0.510 and 0.594, respectively. Both values lie well above the threshold for the transition to the snake state, as deduced from Eq. (16b). Then  $\kappa$  assumes the values  $-0.164$  and  $-0.211$  for the two choices of the fourth-order anisotropy  $k_2$ .

We first examine the solutions for the ground-state magnetization deduced from Eq. (14) by setting the Zeeman field to zero and also we set  $K_2$  to zero for the moment. With  $h_A$  set to 0.0542, we then have only one free parameter,  $h_K$ . We proceed by solving Eq. (14) for various values of  $l$ , and then we search for the value of  $l$  which minimizes the free energy per unit length as given in Eq. (12).

In Fig. 1(a), we show the maximum angular deviation of the magnetization from the  $z$  axis as a function of  $h_K$  in the snake state, and the dimensionless period  $l=L/R$  is illustrated in Fig. 1(b). We see the onset of the snake state at  $h_K=0.27$  as deduced earlier from Eq. (16b), and right at the onset of the instability the period  $l=2.57$  as discussed above. As  $h_K$  increases, the period lengthens. Clearly the uniaxial anisotropy in the nanowire will have to be substantially larger than in bulk Co for the period reported in Ref. 12 ( $l=L/R \sim 15$ ) to be realized.

In Fig. 2, we show the spatial variation in the magnetization for three choices of the dimensionless parameter  $h_K$ . Just above threshold, as demonstrated above, the solution is very similar to the Ansatz set forth in Ref. 14. We see that this is so in the example displayed in Fig. 2(a). However, as we see from Fig. 1(a), the maximum deflection angle in the snake state increases very rapidly to assume large values not far from threshold. As we see from Fig. 2(b), by the time we reach values of  $h_K$  in the range appropriate to bulk Co, the state has a very different character than that envisioned in Ref. 14. We have domains in which the magnetization is canted from the  $z$  axis at close to a constant angle, separated by domain walls. As we see from Fig. 2(c), as  $h_K$  increases, the domains lengthen while the thickness of the walls changes little. The energy per unit length of the domain state is lower in energy than a state in which we have uniform canting of the magnetization, with  $\theta(z)$  constant everywhere.

However, for the larger values of  $h_K$ , when the free energy is plotted as a function of  $l=L/R$  the minimum is very broad indeed. This suggests that the snake state is a very soft and easily deformable state at the larger values of  $h_K$ . High accuracy is required to locate the minimum. For instance, when  $h_K=1$ , the minimum is at  $L/R=8.89$ . The dimensionless free energy per unit length, when compared to that in the ferromagnetic state assumes the value of  $-0.53029$  at the minimum. For  $L/R=9.5$ , the free energy per unit length is only very slightly larger,  $-0.53018$  whereas for  $L/R=7.5$  the free energy per unit length is  $-0.52927$ . It should be noted that

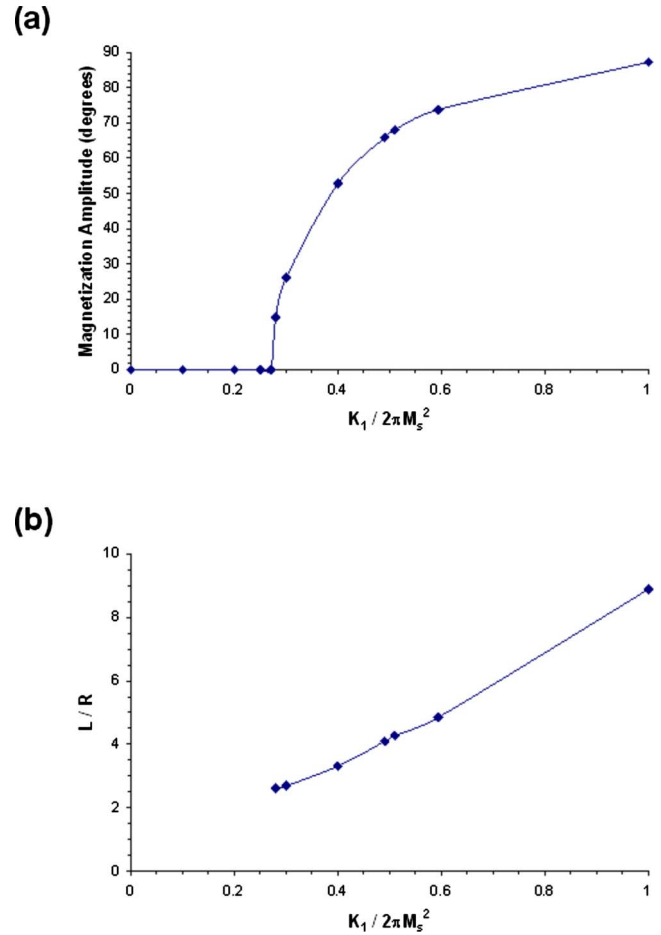


FIG. 1. (Color online) As a function of the dimensionless parameter  $h_K=K_1/2\pi M_s^2$ , we plot (a) the maximum angular deviation from the  $z$  axis realized in the snake state and (b) the period  $L$  as a function of this parameter. The calculations are for a nanowire with radius  $R=40$  nm and exchange strength discussed in the text.

the authors always found magnetic dipoles of opposite polarity at the ends of the wires they probed. This suggests the snake state adjusts itself so such a configuration may be realized. This is compatible with the notion that the minimum in the free energy per unit length is broad and shallow, for wires which exhibit a long period. Earlier experimental studies reported complex domain structures in these wires but not the periodic structure displayed in Ref. 12. Possibly the domains are easily pinned by defects of various sorts.

Addition of the fourth-order anisotropy as described by our parameter  $K_2$  does not greatly change the spatial form of the magnetization realized in the snake state. However, it does decrease both the maximum canting angle and also the period. We illustrate this in Fig. 3, for the case where  $h_K=0.594$ . With parameters appropriate to bulk Co in mind, we have confined our attention to the case where  $K_2 < 0$ .

An interesting question concerns the influence of an externally applied Zeeman field on the snake state. Can one modify its properties through application of only a modest field? This would be highly desirable. One may envision devices based on the propagation of spin waves down a sample in which the snake state is present. If the amplitude of the magnetization or the period can be altered by applica-

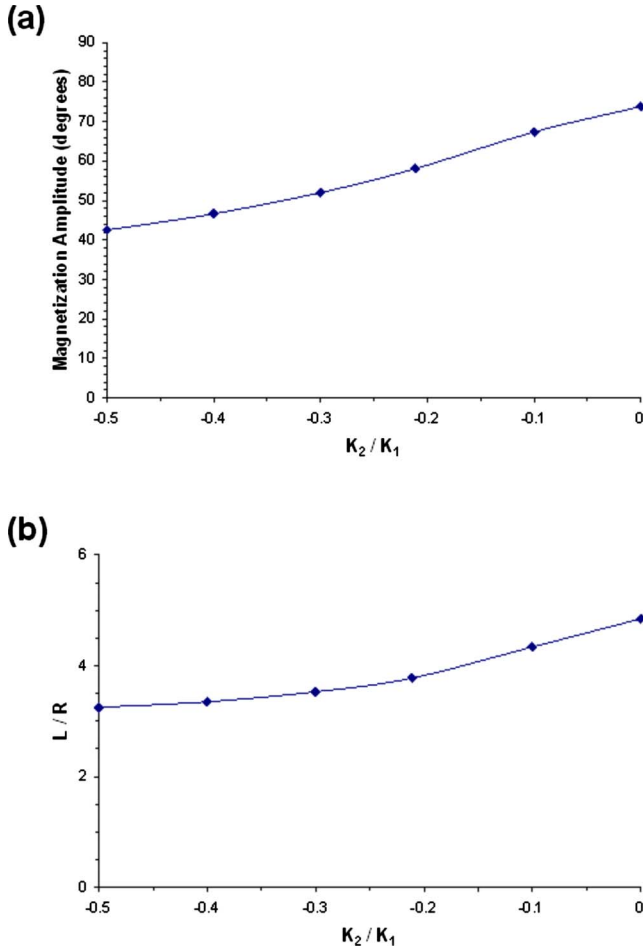


FIG. 3. (Color online) For the case where the second-order anisotropy  $K_1/2\pi M_S^2 = h_K = 0.594$ , we show (a) the maximum deflection angle in the snake state and (b) its period as a function of the strength of the quartic anisotropy  $K_2$ .

tion of a modest field, then the propagation characteristics of the spin waves could be easily altered. The fact that the free energy has the very shallow minimum when calculated as a function of  $L/R$ , as discussed above, suggests the state is “soft” and easily modulated by application of an external magnetic field.

In Fig. 4, we show the maximum angle realized in the snake state, as a function of the strength of a Zeeman field applied parallel to the axis of symmetry of the wire (the  $z$  direction). We have chosen  $h_K = 0.594$  for this calculation; this is a reasonable estimate of the second-order anisotropy one might expect in Co nanowires. Also we have taken  $K_2 = 0$ . A field whose strength is in the range of 0.32 that of  $4\pi M_S$  is sufficient to suppress the snake state, and return the system to a uniform ferromagnetic state. This, for Co, is a field of 0.55 T, which is quite modest. In zero field, for the parameters used in this calculation, one has  $L/R = 4.85$  and the period decreases with magnetic field so that  $L/R$  is about 2.6 before the system returns to the ferromagnetic state. This suggests that application of a modest field parallel to the symmetry axis has a large effect on the snake state. For a field of magnitude of only 0.1 that of  $4\pi M_S$  (0.173 T for Co), the maximum angle in the ground state changes from  $74^\circ$  to

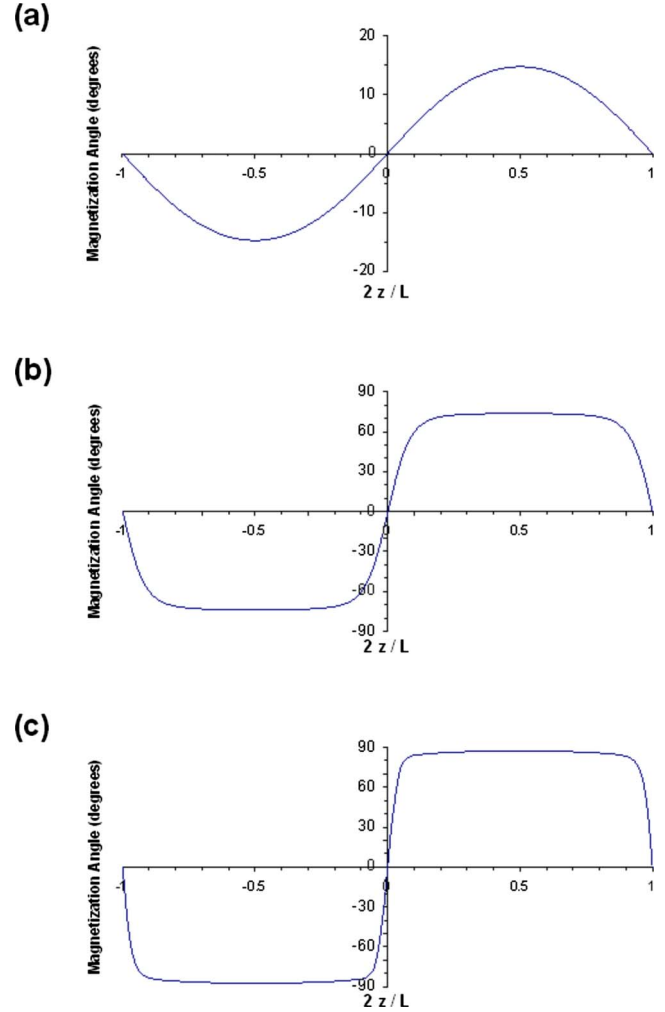


FIG. 2. (Color online) The magnetization profile in the snake state, for three choices of the parameter  $h_K$ . In these calculations, the fourth-order anisotropy described by  $K_2$  has been taken to zero. We show the magnetization profile for (a)  $h_K = 0.28$ , just above the threshold value of 0.27, (b)  $h_K = 0.594$ , appropriate to the case where the nanowire is described by anisotropy in the range of bulk Co values, and (c)  $h_K = 1.0$ .

$57^\circ$ , a change of 23%. Such a field decreases the period from  $L/R = 4.85$  to 3.65.

The soft nature of the snake state can be appreciated through its response to a magnetic field applied perpendicular to the symmetry axis of the wire, and thus parallel to the easy axis. We find that very small applied fields induce a substantial transverse magnetization. The mechanism is field-induced displacement of the domain walls, which leads to an asymmetry in the domain pattern and thus a large transverse moment. For the case where  $h_K = 0.594$  and  $\kappa = 0$  we illustrate this point in Fig. 5. For this choice of anisotropy field, in zero applied field of the ground state, one has  $L/R \approx 5$ .

If we suppose for the nanowire that  $4\pi M_S = 1.73$  T as in bulk Co, then the calculations in Fig. 5(a) correspond to an applied field that is only 173 G and we see a substantial modification of the domain pattern. In Fig. 5(b), the applied field is 865 G. Thus the ground state responds quite dramati-

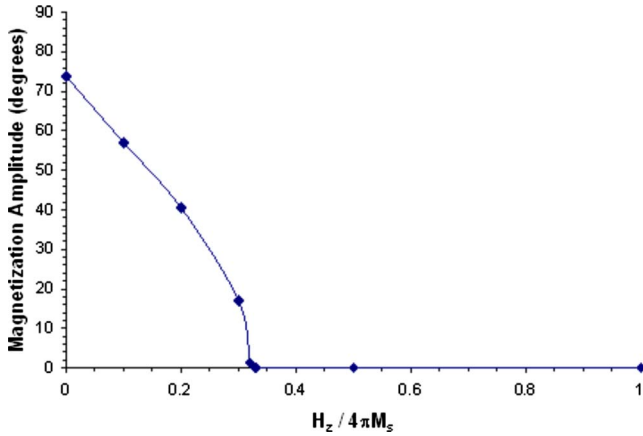


FIG. 4. (Color online) The maximum deviation of the magnetization from the symmetry axis in the snake state, as a function of magnetic field applied parallel to the symmetry axis of the nanowire. For these calculations we have taken  $h_K=0.594$  and  $K_2=0$ .

cally to an applied field of very modest strength. When  $H_0/4\pi M_S=0.01$ , we find for the transverse moment  $M_x=0.15M_S$  while for  $H_0/4\pi M_S=0.05$ , we have  $M_x=0.46M_S$ . The transverse field decreases the moment parallel to the symmetry axis of the wire. When  $H_0/4\pi M_S=0.05$ , the net longitudinal moment is reduced to  $0.88M_S$ . The very large weak-field transverse susceptibility will serve as a signature of the snake state.

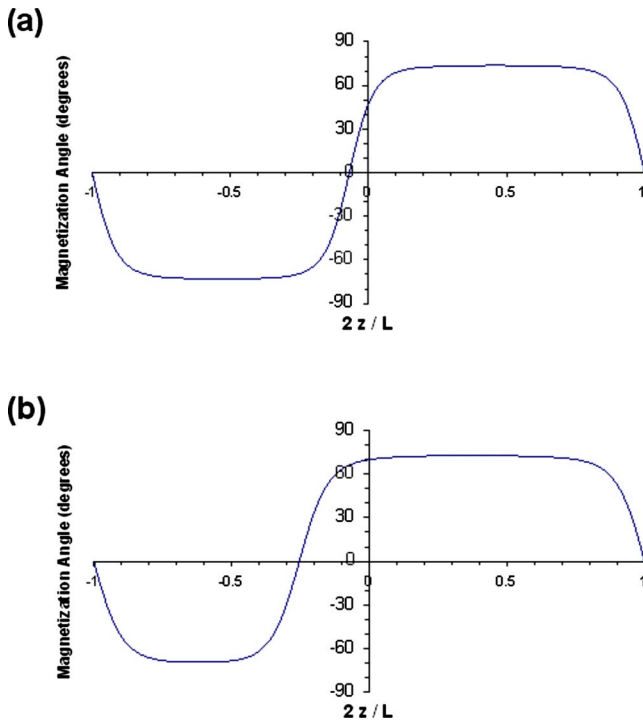


FIG. 5. (Color online) We illustrate the influence of an external magnetic field on the nature of the ground state, for the case where the magnetic field is applied perpendicular to the symmetry axis of the nanowire and parallel to the easy axis. In (a), the strength of the field is  $H_0/4\pi M_S=0.01$  and in (b) the strength is  $H_0/4\pi M_S=0.05$ .

IV. CONCLUDING REMARKS

In this paper, we have developed the theory of the nature of the ground state of a ferromagnetic nanowire in which the easy axis lies within the plane perpendicular to the symmetry axis of the wire. The motivation for our analysis is the synthesis of Co nanowires where such a geometry is realized, as described in Refs. 6–12. The theory presented here, like that also found in Ref. 14, is valid in the limit of small wire radii, by virtue of the assumption that the canting angle  $\theta$  depends only on the coordinate  $z$ , where the  $z$  axis is the symmetry axis of the wire.

For the limit just described, we have obtained a compact representation of the energy per unit length of such a nanowire, for a ground state described by an arbitrary angular deviation  $\theta(z)$  of the magnetization from the symmetry axis. From this functional, we derived an Euler Lagrange equation whose solution yields a description of the ground state. In Sec. III, we discussed the nature of the solutions of this equation, with the assumption that in the ground state  $\theta(z)$  is periodic with  $L$ , found by minimizing the energy per unit length.

The authors of Ref. 14 have also explored this issue in the thin-wire limit examined here, for the case where  $\theta(z)$  is assumed to have the special form  $\theta_0 \sin(2\pi z/L)$ . Here we show analytically that this form emerges from our Euler Lagrange equation just above the threshold value of the transverse anisotropy required to render the ferromagnetic state unstable with respect to the snake state, wherein  $\theta(z)$  is nonzero and periodic. Our numerical work shows that the Ansatz employed in Ref. 14 describes the ground state only very close to threshold. Save for this near-threshold region, the picture of the ground state which emerges is very different. We have domains inside of which the magnetization is canted away from the symmetry axis; the canting angle alternates in sign as one moves from one domain to the next. The domains are then separated by domain walls also of alternating sign, as one moves down the  $z$  axis.

The snake state is a very soft state, most particularly when the transverse anisotropy is sufficiently large that the ratio  $L/R$  is large; the energy per unit length associated with the solution of the Euler Lagrange equation, plotted as a function of  $L/R$  displays a very broad, shallow minimum. A consequence is that the state responds strongly to very small applied magnetic fields. Particularly striking is the large transverse moment induced by a very weak magnetic field applied perpendicular to the symmetry axis of the wire. The state is thus easy to deform with very small fields. A measurement of the low-field transverse susceptibility of the state will be of great interest, in our view.

We shall be interested in the nature of spin waves which can propagate in the snake state. This will be examined in future work. One may expect gaps in the spin-wave dispersion relation, of course, for wave vectors equal to the reciprocal-lattice vector of the ground state. What is intriguing to us is that it should prove easy to modify the spin-wave propagation characteristics in the ground state through application of a very weak field perpendicular to the symmetry axis of the wire. This should prove very interesting from the device point of view.

It is the case that the period we calculate, normalized to the radius of the wire, is considerably smaller than found in the experiments reported in Ref. 12. That this is so is the case if the system parameters are close to those realized in bulk Co metals. We can see from Fig. 1(b) that if the anisotropy in these nanowires is somewhat stronger than that in bulk Co, we can obtain rather large values of  $L/R$ . Thus the measurement of the magnetic properties of these very interesting materials is highly desirable. It is also the case that the details of the ground state realized in any particular sample may be controlled by physics not contained in our analysis. Since the energy minimum is so very shallow for large values of  $L/R$ , the state realized may be very sensitive to defects or, as suggested by the observation of strong magnetic dipoles in

the samples, by end effects. Of course, the use of the thin-wire limit in our description of the ground state may be open to question as well. Further experiments on Co nanowires and hopefully on other materials in which the easy axis is perpendicular to the symmetry axis can provide tests of the basic picture set forth in this paper.

#### ACKNOWLEDGMENTS

We are most grateful to Ilya Krivorotov for numerous very stimulating discussions during the course of this research. The research of D.L.M. was supported by the U.S. Department of Energy through Grant No. DE-FGo3-84ER-45083.

---

\*Corresponding author; Also at P.O. Box 14762, Scottsdale, AZ 85267, USA.

<sup>1</sup>As an example, note the discussion of exotic magnetic states realized in magnetic superlattices given by R. E. Camley, *Nanomagnetism: Ultrathin Films, Multilayers and Nanostructures*, edited by D. L. Mills and J. A. C. Bland (Elsevier, Amsterdam, 2006), p. 77.

<sup>2</sup>See the chapter by A. Fert, A. Barthélémy, and F. Petroff, p. 153 of Ref. 1.

<sup>3</sup>M. Farle, W. Platow, A. N. Anisimov, P. Pouloupoulos, and K. Baberschke, *Phys. Rev. B* **56**, 5100 (1997).

<sup>4</sup>D. P. Pappas, K. P. Kamper, and H. Hopster, *Phys. Rev. Lett.* **64**, 3179 (1990).

<sup>5</sup>U. Ebels, J. L. Duvail, P. E. Wigen, L. Piraux, L. D. Buda, and K. Ounadjela, *Phys. Rev. B* **64**, 144421 (2001).

<sup>6</sup>L. Belliard, J. Miltat, A. Thiaville, S. Dubois, J. L. Duvail, and

L. Piraux, *J. Magn. Magn. Mater.* **190**, 1 (1998).

<sup>7</sup>J. M. García, A. Asenjo, J. Velázquez, D. García, M. Vázquez, P. Aranda, and E. Ruiz-Hitzky, *J. Appl. Phys.* **85**, 5480 (1999).

<sup>8</sup>J.-E. Wegrowe, D. Kelly, A. Franck, S. E. Gilbert, and J.-Ph. Ansermet, *Phys. Rev. Lett.* **82**, 3681 (1999).

<sup>9</sup>M. García, A. Asenjo, M. Vaquez, P. Aranda, and E. Ruiz-Hitzky, *IEEE Trans. Magn.* **36**, 2981 (2000).

<sup>10</sup>J. M. García, A. Thiaville, and J. Miltat, *J. Magn. Magn. Mater.* **249**, 163 (2002).

<sup>11</sup>H. Zeng, R. Skomski, L. Menon, Y. Liu, S. Bandyopadhyay, and D. J. Sellmyer, *Phys. Rev. B* **65**, 134426 (2002).

<sup>12</sup>Z. W. Liu, P. C. Chang, C. C. Chang, E. Galaktionov, G. Bergmann, and J. G. Lu, *Adv. Funct. Mater.* **18**, 1573 (2008).

<sup>13</sup>A. Fert and L. Piraux, *J. Magn. Magn. Mater.* **200**, 338 (1999).

<sup>14</sup>G. Bergmann, J. G. Lu, Y. Tao, and R. S. Thompson, *Phys. Rev. B* **77**, 054415 (2008).